Sun et al. *Zool. Res.* 2023, 44(1): 78−89
https://doi.org/10.24272/j.issn.2095-8137.2022.274

ZR | Zoological Research

Article Open Access

Whole-genome resequencing reveals recent signatures of selection in five populations of largemouth bass (*Micropterus salmoides*)

Cheng-Fei Sun[1,#], Xin-Hui Zhang[2,3,#], Jun-Jian Dong[1], Xin-Xin You[2,3], Yuan-Yuan Tian[1], Feng-Ying Gao[1], He-Tong Zhang[1], Qiong Shi[2,3,*], Xing Ye[1,*]

[1] *Key Laboratory of Tropical and Subtropical Fishery Resources Application and Cultivation*, *Ministry of Agriculture and Rural Affairs*, *Pearl River Fisheries Research Institute*, *Chinese Academy of Fishery Sciences*, *Guangzhou*, *Guangdong* 510380, *China*

[2] *Shenzhen Key Lab of Marine Genomics*, *Guangdong Provincial Key Lab of Molecular Breeding in Marine Economic Animals*, *BGI Academy of Marine Sciences*, *BGI Marine*, *Shenzhen*, *Guangdong* 518081, *China*

[3] *College of Life Sciences*, *University of Chinese Academy of Sciences*, *Beijing* 100049, *China*

ABSTRACT

Largemouth bass (*Micropterus salmoides*) is an economically important fish species in North America, Europe, and China. Various genetic improvement programs and domestication processes have modified its genome sequence through selective pressure, leaving nucleotide signals that can be detected at the genomic level. In this study, we sequenced 149 largemouth bass fish, including protospecies (imported from the US) and improved breeds (four domestic breeding populations from China). We detected genomic regions harboring certain genes associated with improved traits, which may be useful molecular markers for practical domestication, breeding, and selection. Subsequent analyses of genetic diversity and population structure revealed that the improved breeds have undergone more rigorous genetic changes. Through selective signal analysis, we identified hundreds of putative selective sweep regions in each largemouth bass line. Interestingly, we predicted 103 putative candidate genes potentially subjected to selection, including several associated with growth (p*sst1* and *grb10*), early development (*klf9*, *sp4*, and *sp8*), and immune traits (*pkn2*, *sept2*, *bcl6*, and *ripk2*). These candidate genes represent potential genomic landmarks that could be used to improve important traits of biological and commercial interest. In summary, this study provides a genome-wide map of genetic variations and selection footprints in largemouth bass, which may benefit genetic studies and accelerate genetic improvement of this economically important fish.

Keywords: Largemouth bass; Whole-genome

Received: 24 August 2022; Accepted: 01 November 2022; Online: 02 November 2022

Foundation items: This study was supported by the Key-Area Research and Development Program of Guangdong Province (2021B0202020001), China Agriculture Research System of MOF and MARA (CARS-46), Central Public-interest Scientific Institution Basal Research Fund of CAFS (2020TD23, 2020ZJTD-02), Project of Construction of Guangdong Aquatic Seed Industry Demonstration Base 2021, and Special Funds for Science Technology Innovation and Industrial Development of Shenzhen Dapeng New District (KJYF202101-02)

#Authors contributed equally to this work

*Corresponding authors, E-mail: shiqiong@genomics.cn; gzyexing@163.com

resequencing; Signatures of selection; Growth; Immunity

INTRODUCTION

Some 10 000 years ago, humans began to domesticate animals and plants to meet their food requirements (Chen et al., 2022). Domestication is a sustained multi-generational process, in which humans exercise a significant degree of control over the reproduction and care of a target organism to secure a more predictable supply of resources from the species (Zeder, 2015). Humans also induce further gradual changes in species once they are domesticated (Saraiva et al., 2018). With each generation in the domestication process, target animals become increasingly suited to captive conditions and human requirements. Fish domestication is a dynamic and persistent process that begins as soon as individuals are transferred from the wild into captive conditions (Teletchea, 2015). In most cases, domestication allows fish to adapt to captive conditions continuously, with the goal of modifying selected traits to produce more productive and efficient individuals (Teletchea, 2021).

At present, animal domestication studies have primarily focused on population genetics, using genetic polymorphic markers to examine relationships between domestic animals and their wild ancestors or potential domestication events (Larson & Burger, 2013). Population genetics typically examines genetic differences within or between populations and is differentiated from phenotypic approaches in evolutionary modeling by emphasizing genetic phenomena such as dominance, epistasis, selective signals, degree to which linkage disequilibrium is broken by genetic recombination, and genetic diversity (Tang, 2020). With the rapid development of next-generation sequencing technologies, single nucleotide polymorphism (SNP)-based genomic variation is often applied in population genetics and animal domestication research. Mäkinen et al. (2015) analyzed genome-wide SNPs from three domesticated Atlantic salmon strains and wild conspecifics to identify potential loci underpinning domestication and identified several loci with footprints of selection localized in different linkage groups between wild populations and hatchery strains. Based on 9 827 genome-wide SNPs, Nayfa et al. (2020) investigated the population genetic structure and signatures of selection in a domesticated Abbassa strain compared to eight wild Nile tilapia populations from Egypt and highlighted the importance of domestication as well as wild population structure for future management and disease prevention.

Largemouth bass (*Micropterus salmoides*), belonging to Perciformes, Centrarchidae, and Micropterus. It is native to North American freshwater waters and is an important game fish. In the late 1970s, it was introduced to Taiwan of China from US, and with successful culture achieved in 1983. The fish was subsequently introduced from Taiwan to Guangdong Province in mainland China, where it has become an important freshwater aquaculture species due to its tender meat, lack of intermuscular bones, wide growth temperature, fast growth rate, and easy fishing (Sun et al., 2021). We recently reported a chromosome-level genome assembly of *M. salmoides* based on PacBio and Hi-C sequencing (Sun et al., 2021). However, genomic breeding of *M. salmoides* has not yet been reported. To elucidate the genetic basis of its domestication, understand the impact of directed breeding on its genomic variation, and explore how directed breeding can be accelerated, we performed whole-genome resequencing of five different populations, including a wild population introduced from the US (WL), two cultured populations from Taiwan (TWL) and mainland China (TL), and two representative selected populations from Guangdong (Youlu (YL) and Jiadefeng (JDF)). Population genetic analysis and selection signal localization were carried out to explore the genomic differences among the five populations.

MATERIALS AND METHODS

Ethics approval and consent to participate

All fish-used experiments were conducted in accordance with the specific guidelines on the care and use of animals for scientific purposes as outlined by the Institutional Animal Care and Use Committee (IACUC) of the Pearl River Fisheries Institute, Chinese Academy of Fishery Sciences (CAFS), China. The IACUC approved this study under the CAFS project “Breeding of LMB-2019”.

Fish sampling

The US-introduced protospecies (WL, 29 individuals) was obtained from Anhui Zhanglin Fishery Co., Ltd. (Tongling, Anhui, China), the Taiwan breeding population (TWL, 30 individuals) was obtained from Guangzhou Huaxuan Aquatic Co., Ltd. (Guangzhou, Guangdong, China), the Youlu breeding population (YL, 30 individuals) was provided by Aiyu Breeding Co., Ltd. (Guangzhou, Guangdong, China), and the common breeding population (TL, 30 individuals) and Jiadefeng breeding population (JDF, 30 individuals) were obtained from the conservation and breeding population of Foshan Xinrong Aquatic Co., Ltd. (Guangzhou, Guangdong, China). Caudal fins were collected and stored in 95% ethanol at –20 °C for DNA extraction.

Whole-genome resequencing

Genomic DNA was extracted from fish fins using a QIAamp DNA Mini Kit (Qiagen, USA) following the manufacturer’s instructions. DNA quality was determined via agarose gel electrophoresis and an Agilent 4200 Bioanalyzer (Agilent Technologies, USA). Ten Illumina paired-end DNA libraries with an insert size of 350 bp were constructed using a Genomic DNA Sample Prep Kit (Illumina, USA) following the manufacturer’s protocols, then sequenced on the Illumina NovaSeq 6000 platform (USA) in paired-end mode (2× 150 bp).

Read trimming and variant calling

Raw reads with adaptors and low-quality bases were removed using SOAPnuke (-n 0.1 -l 5 -q 0.5) (Chen et al., 2018). The clean reads were mapped to the largemouth bass reference genome from NCBI (No. ASM1485139v1; Sun et al., 2021) using Burrows-Wheeler Aligner (BWA) v0.7.15 with default parameters (Li & Durbin, 2009). Mapping results were then converted into BAM format and sorted with SAMtools v1.3.1

(Li et al., 2009). Duplicate reads were removed using Picard v1.54 (https://broadinstitute.github.io/picard/). If multiple read pairs were mapped to the same sequence, only the pair with the highest mapping quality was retained.

Variant calling of SNPs and indels was performed using the Genome Analysis Toolkit (GATK) v4.0 (Franke & Crowgey, 2020). The SNPs were filtered using the following criteria: (i) SNPs with QD<2.0, FS>60.0, MQ<40.0, MQRankSum<-12.5, and ReadPosRankSum<-8.0; (ii) variant missing rate less than 0.1 and coverage depth >4 and <100; (iii) minor allele frequency (MAF) >0.05; and (iv) linkage disequilibrium pruning, performed using PLINK v1.9 (Purcell et al., 2007) with a window size of 10 kb, step size of one SNP, and r^2 threshold of 0.5. Subsequently, we annotated and predicted the effects of filtered SNPs using snpEff v4.3 (Cingolani et al., 2012). We constructed the snpEff databases using GFF3 and FASTA files from the largemouth bass genome assembly (Sun et al., 2021).

Phylogeny and population genetic structure

Filtered SNPs were used for phylogenetic analysis. A neighbor-joining (NJ) phylogeny was constructed with 100 bootstraps using PHYLIPNEW v3.69 (https://emboss.open-bio.org/pub/EMBOSS/). The NJ tree was rooted with the outgroup of 29 WL and visualized using FigTree v1.4.3 (http://tree.bio.ed.ac.uk/software/figtree/). The phylogenetic tree was then polished using iTOL v6.4.3 (Letunic & Bork, 2021). Principal component analysis (PCA) of whole-genome SNPs was performed using FlashPCA v1.2.6 (Abraham & Inouye, 2014) and population structure was analyzed using ADMIXTURE v1.3.0 (Alexander et al., 2009). The likelihood of ancestral kinship (*K*) from 2 to 6 was tested using all SNPs.

We compared linkage disequilibrium (LD) patterns among different groups identified based on domestication type. LD decay was measured by calculating correlation coefficients (r^2) for all pairs of SNPs within 500 kb using PopLDdecay v3.40 (Zhang et al., 2019a).

Nucleotide diversity and fixation index analysis

Genetic diversity between populations was calculated based on observed and expected heterozygosities (Ho and He) using PLINK v1.90 (Purcell et al., 2007). Nucleotide diversity (π) and fixation index (*F*st) were calculated using VCFtools (Danecek et al., 2011) with a sliding window of 100 kb and step size of 10 kb (–window-pi 100000 –window-pi-step 10000). The levels of genetic differentiation represented by *F*st values (from 0 to 1) were rated as *F*st>0.25 (huge differentiation), 0.15 to 0.25 (great differentiation), 0.05 to 0.15 (moderate differentiation), and *F*st<0.05 (negligible differentiation) (Choy et al., 2015). Huge differentiation implied considerable separation between two populations, while negligible differentiation implied little divergence and free dispersal between two populations.

Detection of selective signatures

Genome-wide scanning of selective sweeps during domestication and artificial breeding was performed by comparing allele frequency between farmed (JDF, YL, TL and TWL) and introduced (WL) populations of largemouth bass using three approaches, i.e., ratio of π, *F*st, and cross-population extended haplotype homozygosity (XP-EHH). For definitions, π is the expected heterozygosity of each locus derived from the average number of sequence differences in a set of samples; *F*st is the inbreeding coefficient of a subgroup, used to estimate pairwise gene composition of candidate genes between paired subgroups (Lu et al., 2019); and XP-EHH compares haplotype lengths of populations to detect selective scanning when alleles are close to or fixed in one population but remain polymorphic in another (Sabeti et al., 2007), calculated using selscan v1.3.0 with default parameters (Szpiech & Hernandez, 2014) and genetic distance using published data (Dong et al., 2019). The standard parameters of selscan were used to normalize the original XP-EHH values. The π ratio, *F*st, and XP-EHH values were sorted from large to small, with the top 5% taken as the significant threshold line to judge whether selection occurred among the examined populations and to screen selected gene intervals. Windows identified by all three methods were recognized as putative selection sweeps. Finally, the predicted candidate genes were subjected to functional enrichment analysis using the Gene Ontology (GO) and Kyoto Encyclopedia of Genes and Genomes (KEGG) databases.

RESULTS

Summary of whole-genome resequencing and variation calling

Whole-genome resequencing of the 149 individuals from one wild (WL; *n*=29) and four breeding populations (JDF, YL, TL, and TWL; *n*=30 for each population) generated a total of 11.2 billion 150 bp paired-end reads (1.68 Tb in total), with an average depth of 11.77× per individual. After filtering, 1.67 Tb of clean data were obtained. We subsequently aligned clean reads to the largemouth bass reference genome (Sun et al., 2021). The mapping rates varied from 94.94% to 99.44%, and average depth of effective mapped reads was 11× (ranging from 9.77× to 12.36×). After applying basic filtering criteria (see Materials and Methods), a total of 3 615 413 SNPs (including 1 908 815 in JDF, 1 999 614 in YL, 1 850 090 in TL, 1 650 264 in TWL, and 2 782 319 in WL) and 865 493 indels were obtained (Figure 1). SNPs were further filtered, with 2 289 125 high-quality SNPs finally retained for further analysis.

The WL population had a significantly higher number of SNPs compared to the other four populations. A survey of all identified SNPs in the largemouth bass genome showed that every chromosome contained regions of high SNP density, with significant deviations from the whole-genome average. In total, 36.7% of identified SNPs were localized in intergenic regions, 40.8% were localized in intron regions, and 2.8% were localized in coding sequences. The nonsynonymous-to-synonymous substitution ratio for the SNPs in the coding regions was 0.72 (Supplementary Table S1).

Population phylogeny and structure

The filtered SNPs were used to analyze phylogeny and population structure. The NJ tree showed that JDF and YL populations and the TL and TWL populations clustered together with small genetic distances (0.24 and 0.211, respectively), whereas the WL population appeared as a

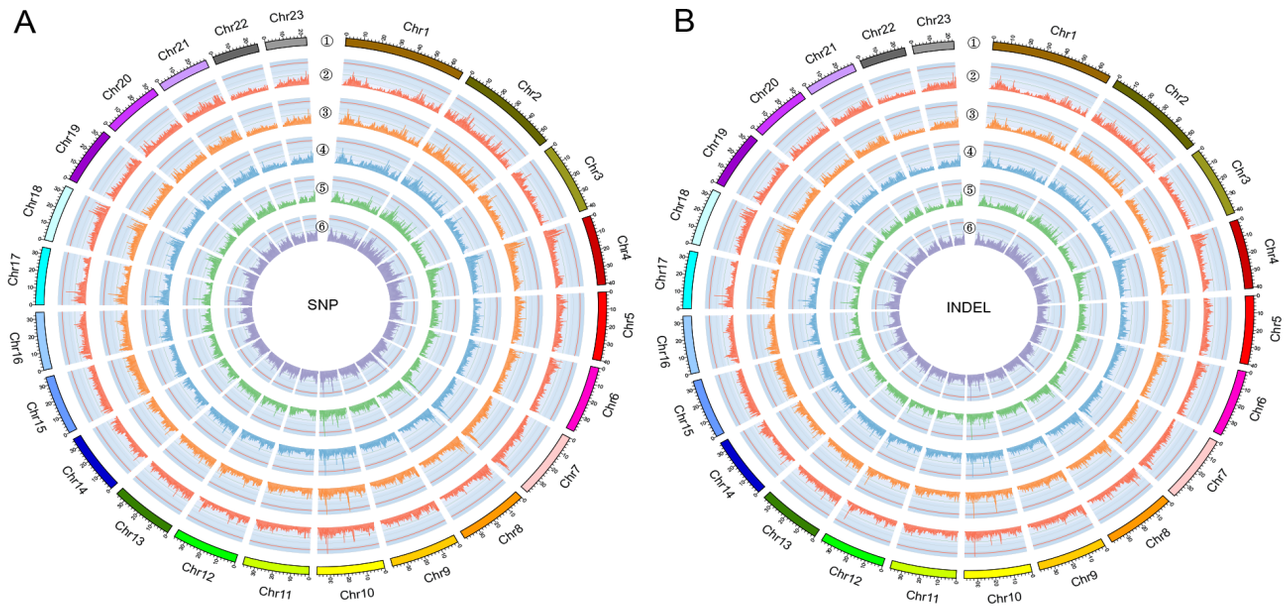

Figure 1 Density of SNPs and indels in various chromosomes

A: SNP distribution in each 100 kb genomic interval. B: Indel distribution in each 100 kb genomic interval. From outside to inside: 1 represents chromosomes and 2 to 6 represent JDF, YL, TL, TWL, and WL populations, respectively.

single group, suggesting a higher level of diversity and larger genetic distance (0.363 on average; Figure 2A). This finding was supported by PCA, which demonstrated that the WL population was more differentiated than the JDF, YL, TL, and TWL populations (Figure 2B). ADMIXTURE-based population structure analysis generated similar results. Error was smallest (0.48392) when clusters were set to K=4 (Supplementary Figure S1), and all populations converged to four clusters with the highest average likelihood value (Figure 2C). The WL population exhibited more admixed and diversified genetic components than the other two clusters.

Comparison of LD and genetic diversity

Characterization of LD patterns is crucial for genetic studies. We analyzed LD (measured as r^2) in the population genomes. The physical distances between SNPs (half of the maximum value) were 3.06 kb (r^2=0.450), 1.78 kb (r^2=0.448), 3.36 kb (r^2=0.452), 8.71 kb (r^2=0.458), and 142 bp (r^2=0.451) for the JDF, YL, TL, TWL, and WL populations, respectively. The four breeding populations showed slow decay rates and high levels of LD, whereas the WL population exhibited a rapid decay rate and low level of LD (Figure 3A), indicating the lowest selective pressure and highest genetic diversity compared to the other four populations.

Average genome-wide π in the JDF, YL, TL, TWL, and WL populations was 7.17×10^{-4}, 7.37×10^{-4}, 6.62×10^{-4}, 6.05×10^{-4}, and 7.00×10^{-4}, respectively. The π values were significantly different between WL and the other four populations (P<0.05, Figure 3B). The YL population had the highest π value, while the TWL population had the lowest, suggesting that the latter could undergo rigorous domestication or improvement.

The Fst values between WL and the other four populations were similarly high: $F\text{st}_{(\text{WL vs. JDF})}$=0.206, $F\text{st}_{(\text{WL vs. YL})}$=0.198, $F\text{st}_{(\text{WL vs. TL})}$=0.22, and $F\text{st}_{(\text{WL vs. TWL})}$=0.242. All Fst values were >0.15 (Figure 3C), implying considerable separation between WL and the other populations.

The Ho/He values for the JDF, YL, TL, TWL, and WL populations were 0.287/0.285, 0.303/0.296, 0.267/0.266, 0.244/0.242, and 0.294/0.300, respectively. The highest Ho and He values were found in the YL and WL populations, respectively, while the lowest values were found in the TWL population (Figure 3D). Thus, the TWL population may have lost substantial genetic diversity due to inbreeding or founder effects.

Selective signals produced by domestication and improvement

To explore potential genomic modifications that occurred during domestication and improvement, we applied an integrated approach combining ($\log_2$ (π ratio), Fst, and XP-EHH (see Materials and Methods) to identify candidate genes for the divergence of WL and the other four populations.

Genome-wide annotated SNPs were used to calculate π ratios between WL and other populations (100 kb windows with 10 kb steps). Genomic loci with significantly high (top 5%) π ratios ($\log_2$ (WL/JDF π ratio)>1.77, $\log_2$ (WL/YL π ratio)>1.417, $\log_2$ (WL/TL π ratio)>1.856, and $\log_2$ (WL/TWL π ratio)>3.108) were identified as highly divergent (Supplementary Figure S2). Subsequently, we identified 338 selected regions containing 1 896 genes in JDF/WL, 383 selected regions containing 2 132 genes in YL/WL, 404 selected regions containing 2 283 genes in TL/WL, and 325 selected regions containing 2 191 genes in TWL/WL.

We calculated global genome Fst values between WL and other populations using a sliding window of 100 kb and shift of 10 kb, and identified 410, 394, 371, and 326 putatively selected genomic regions in the top 5% of Fst: $F\text{st}_{(\text{JDF vs. WL})}$> 0.39, $F\text{st}_{(\text{YL vs. WL})}$>0.38, $F\text{st}_{(\text{TL vs. WL})}$>0.43, and $F\text{st}_{(\text{TWL vs. WL})}$> 0.47 (Supplementary Figure S3), comprising 1 896, 2 132, 2 283, and 2 191 genes in JDF/WL, YL/WL, TL/WL, and

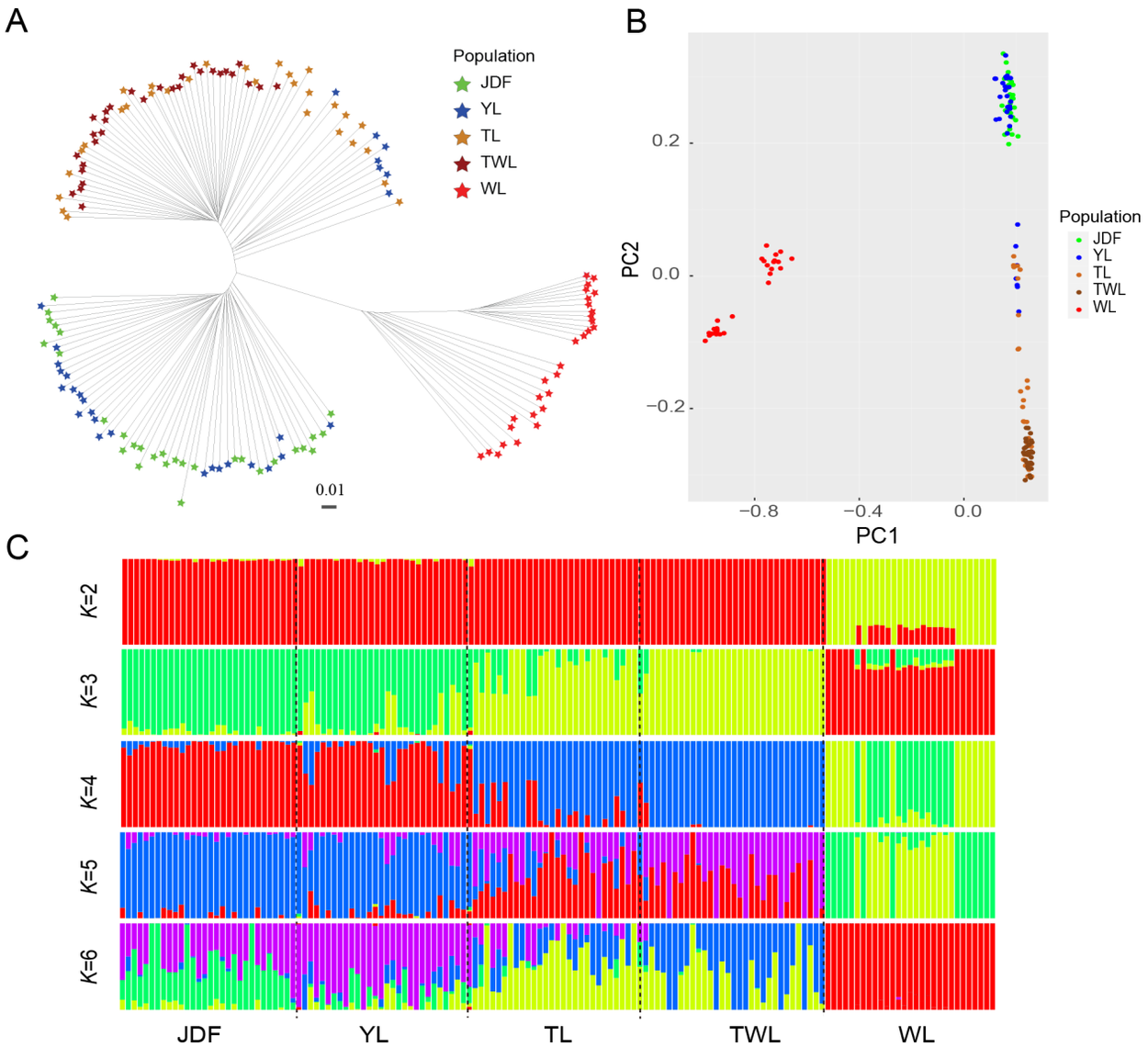

Figure 2 Summary of population structure

A: Phylogenetic tree. B: PCA. C: Population structure. Colors in each fragment represent the proportion of *K*=2~6 ancestral populations assigned to individual genomes. Each accession is represented by a bar, and the length of each colored segment in the bar represents the proportion contributed by that ancestral population.

TWL/WL, respectively.

We scanned genomic regions with extreme allele frequency differentiation and calculated the top 5% of XP-EHH values ($XP\text{-}EHH_{(JDF\ vs.\ WL)}$>1.88, $XP\text{-}EHH_{(YL\ vs.\ WL)}$>1.84, $XP\text{-}EHH_{(TL\ vs.\ WL)}$>1.84 and $XP\text{-}EHH_{(TWL\ vs.\ WL)}$>1.88) as significantly different windows (Supplementary Figure S4). We identified 3 003, 3 462, 3 758, and 3 313 candidate genes in JDF/WL, YL/WL, TL/WL, and TWL/WL, respectively.

The three approaches were combined to identify a total of 477 candidate genes in JDF/WL (Figure 4A), 547 candidate genes in YL/WL (Figure 4B), 363 candidate genes in TL/WL (Figure 4C), and 564 candidate genes in TWL/WL (Figure 4D). Among them, 103 candidate genes were overlapping, while 136, 189, 52, and 362 genes were unique to JDF, YL, TL, and TWL, respectively, compared to the WL population (Figure 4E). The 103 overlapping genes were subjected to functional annotation, with many genes found to be potentially associated with the domestication process. Among these selected genes, several are involved in immune responses, growth, early development, and reproduction (Supplementary Table S2).

DISCUSSION

In this study, we compared a wild population (WL, introduced from the US) and four farmed populations (JDF, YL, TL, and TWL from China) of largemouth bass based on genetic diversity, population structure, and selective signals, with a focus on genomic variations.

Previous studies have identified selection signatures in several aquaculture fish species, including large yellow

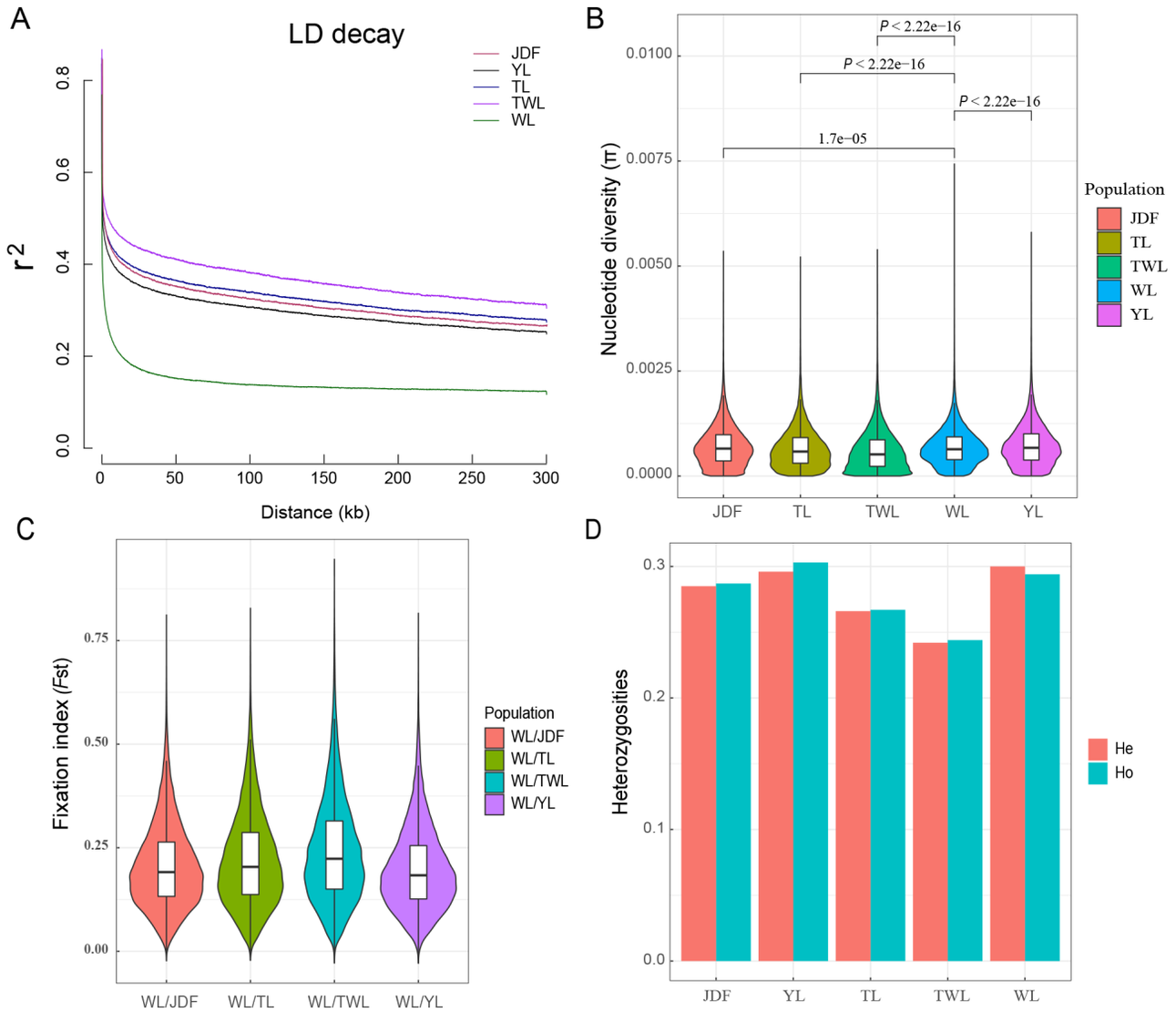

Figure 3 Comparisons of LD and genetic diversity among five examined populations

A: LD decay across studied populations. B: Violin plot of π for each population in 100 kb windows with 10 kb steps. C: Violin plot of *F*st for each population in 100 kb windows with 10 kb steps. D: Heterozygosities of SNPs in five examined populations.

croaker (Kon et al., 2021), Amur ide (Wang et al., 2021a), Atlantic salmon (Gutierrez et al., 2016; López et al., 2019), Nile tilapia (Cádiz et al., 2020; Nayfa et al., 2020), and brown trout (Lemopoulos et al., 2018). To date, however, genomic selection signatures of the largemouth bass have not been reported. Here, we evaluated the presence of genetic diversity and selection signatures in five largemouth bass populations using routine whole-genome resequencing technology.

Genetic diversity and population structure among five examined populations

We evaluated genetic diversity among the five populations based on SNP, π, Ho, and He data. Compared with other aquaculture fish species, largemouth bass exhibited low genetic diversity. For the largemouth bass, we obtained low values of He (ranging from 0.2 to 0.3; Figure 3D) and π (ranging from 6.05 to 7.37×10^{-4}; Figure 3B). In contrast, previous studies have reported He values of 0.2 to 0.4 and π values of 8.46 to 9.39×10^{-4} in Nile tilapia (Van Bers et al., 2012; Yoshida et al., 2019), as well as He values of 0.361 to 0.434 in *Piaractus mesopotamicus* (Mastrochirico-Filho et al., 2019) and 0.664 to 0.912 in wild Chinese sea bass (Wang et al., 2021b).

Low genetic diversity is expected in domesticated populations due to the absence of gene flow from other populations and selective breeding (Baumung et al., 2004). In the five examined largemouth bass populations, we observed higher levels of π (7.17, 7.37, and 7.00×10^{-4}), heterozygosity (0.287/0.285, 0.303/0.296, and 0.294/0.300), and SNPs (1.90, 1.99, and 2.78 million) in the JDF, YL, and WL populations, but lower levels of π (6.62 and 6.05×10^{-4}), heterozygosity (0.267/0.266 and 0.244/0.242), and SNPs (1.85 and 1.65 million) in the TL and TWL populations. These differences in the TL and TWL populations may be due to their different genetic status when first introduced from the US or previous

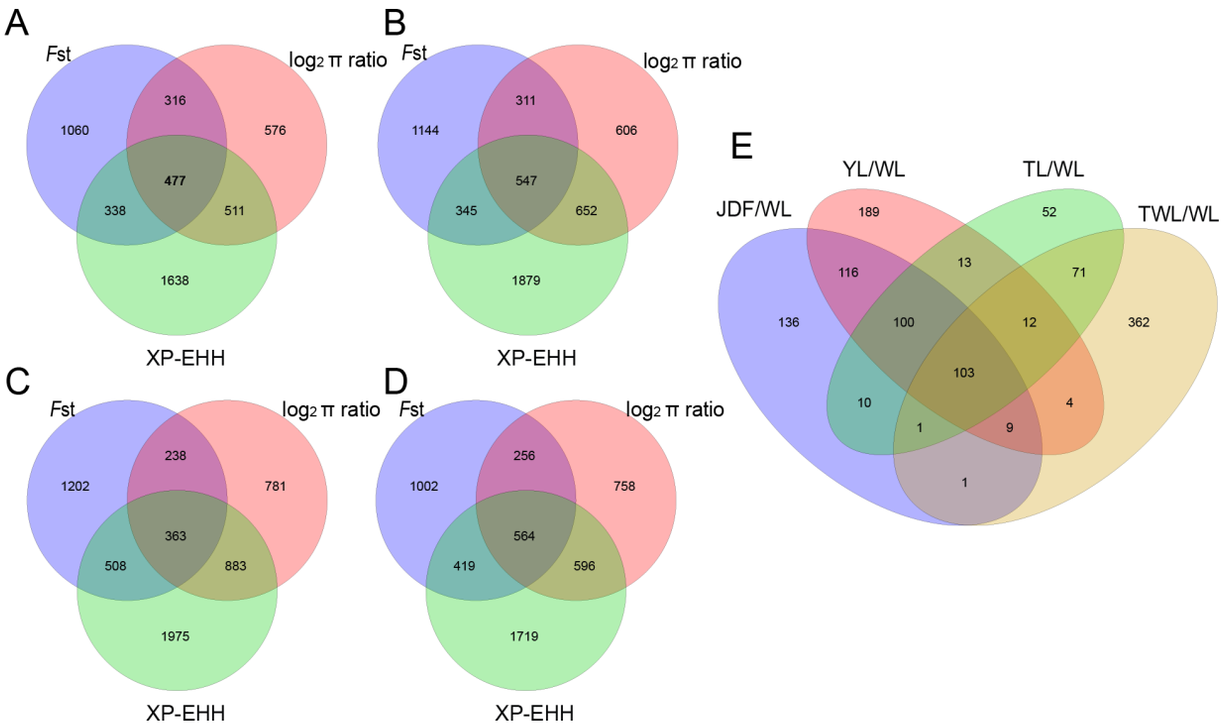

Figure 4 Venn diagrams of shared genes identified by integration of π ratio, XP-EHH, and *F*st approaches in five examined populations

Candidate genes identified in: A: JDF/WL; B: YL/WL; C: TL/WL; D: TWL/WL; and E: combination of π ratio, XP-EHH, and *F*st approaches in four populations compared to the WL population.

artificial breeding experience, resulting in a loss of genetic diversity. Compared with the WL population (introduced from the US), the domestic populations (TL and TWL) showed lower genetic diversity (Figure 3B), consistent with previous reports (e.g., Bai et al., 2008).

We also characterized the genetic relationships and population structure of the five largemouth bass populations using NJ phylogeny and PCA. The NJ phylogenetic tree clustered samples using average genetic distances, and the topology clearly separated the five populations into three groups (Figure 2A). A similar population structure was produced with PCA and admixture analysis (Figure 2B, C). Thus, results showed that the JDF and YL populations (except for six individuals) and the TL and TWL populations were closely related, with apparent differentiation from the WL population.

Selection signals under breeding improvements

We investigated selection signals in five largemouth bass populations using three integrated methods (π ratio, XP-EHH, and *F*st) to search their genomes and highlight genetic variants for the development of productive breeds. In addition, we performed three comparable selective sweep tests to cover genome-wide regions to capture the maximum number of candidate genes and annotate their biological functions.

As expected, our results indicated that domestication and selective breeding have generated changes in the genomes of the studied populations. Based on analysis, we predicted several genes that may be involved in biological processes such as growth, early development, reproduction, immunity, behavior, and environmental adaptation (Figure 5), and may be under pressure from domestication and direct selection.

Growth rate is of economic importance to farmers and easily recorded when breeding candidate animals (Gjedrem & Robinson, 2014). Most genetic improvement projects in aquatic species have focused on growth-related traits (Li et al., 2018; Tsai et al., 2015; Yin et al., 2021; Zhang et al., 2018). In the present study, we identified several candidate genes (Supplementary Table S2) and enriched terms related to growth. For instance, we found that preprosomatostatin 1 (*psst-1*), a precursor of somatostatin (*sst*), was localized in chromosome 3 (Chr3; Figure 6A, C, E). Previous studies have shown that *sst* plays an important role in vertebrate growth regulation by inhibiting growth hormone (*gh*) and insulin-like growth factor 1 (*igf-1*) (Brazeau et al., 1973; Ye et al., 2005; Gahete et al., 2009; Wang et al., 2014). In hungry or immature fish (such as salmon), *sst* is negatively correlated with *igf-1* levels, and stimulative transcription of *sst* in the hypothalamus can block IGF-1 expression in the liver (Sheridan et al., 1998). In addition, *sst* can suppress many pituitary hormones (including thyroid stimulating hormone, adrenocorticotropic hormone, prolactin, secretin, ghrelin, and gallbladder contraction) and gastrointestinal peptides (Ben-Shlomo & Melmed, 2010; Nelson & Sheridan, 2005), and can inhibit insulin (*ins*), glucagon, endocrine gland pancreatic polypeptides, and exocrine gland digestive enzymes to regulate body growth (Cervia & Bagnoli, 2007). Growth factor receptor-bound protein 10 (*grb10*), an insulin receptor-binding protein, can interact with insulin receptors and insulin-like growth-factor receptors (Frantz et al., 1997; He et al., 1998). Overexpression of certain isoforms of the encoded protein

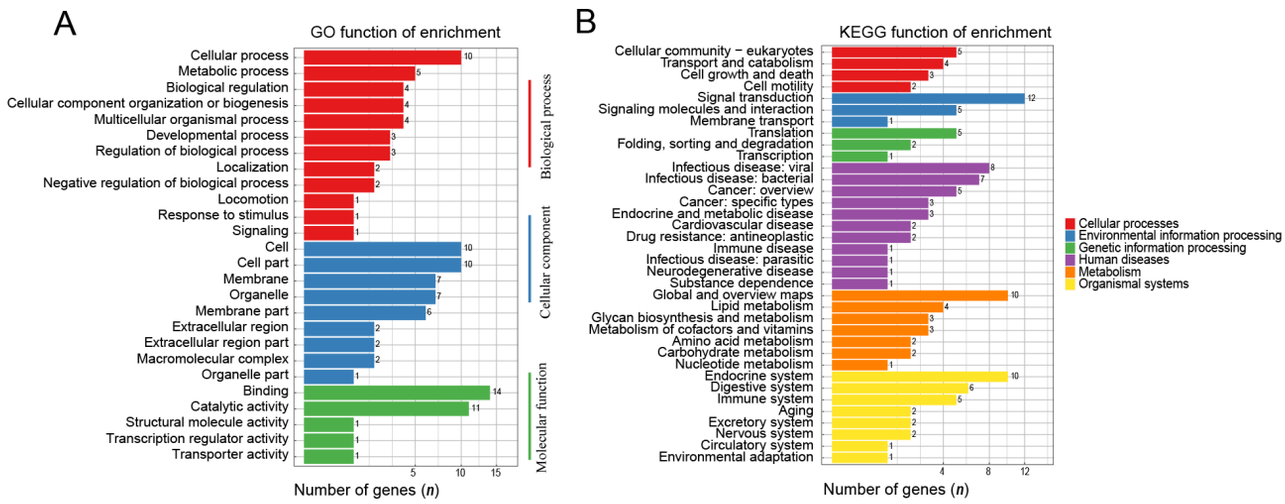

Figure 5 Functional annotation of 103 overlapping genes

A: GO enrichment. B: KEGG enrichment.

inhibits tyrosine kinase activity, leading to growth suppression (Liu & Roth, 1995). In the present study, the SNP genotype of the *grb10* gene (localized in Chr17) was significantly changed in the WL population compared to the four farmed populations (Figure 6B, D, F). In addition, we detected several other candidate genes, such as breast cancer anti-estrogen resistance protein 1 (*bcar1*), cyclic AMP-responsive element-binding protein 5 (*creb5*), and small conductance calcium-activated potassium channel protein 2 (*kcnmb2*), associated with growth hormone synthesis and secretion and insulin secretion.

The Krüppel-like factor (*klf*) and specificity protein (*sp*) transcription factor family play key roles in critical biological processes, including stem cell maintenance, cell proliferation, embryonic development, tissue differentiation, metabolism, and growth (Kawakami et al., 2004; Presnell et al., 2015; Suske, 1999; Yu et al., 1999). In the present study, three KLF/SP transcription factor-related genes (*klf9*, *sp4*, and *sp8*) were identified within the selection region. Knockout of *sp4* can lead to growth retardation and male infertility in mice (Supp et al., 1996). Furthermore, *sp8* regulates fibroblast growth, expression of factor 8 (*fgf8*), and limb outgrowth in zebrafish embryos (Kawakami et al., 2004).

Resistance to infectious diseases is another economically important factor, and the consequences of this trait include fish health and growth (Suebsong et al., 2019; Tran et al., 2015). In largemouth bass, several breeding programs have been applied to select for disease resistance (Duan et al., 2022; Xu et al., 2021). In the current study, we predicted selection in several molecules associated with immune traits. Four genes putatively associated with defense against bacterial pathogens were identified on chromosome 14 (located at 21.8–22.2 Mb). Receptor-interacting serine/threonine kinase 2 (*ripk2*) and serine/threonine-protein kinase N2 (*pkn2*) play critical roles in vertebrate innate immune responses (Liu et al., 2018; McCubrey et al., 2000; Ravichandran et al., 2020). B-cell lymphoma-6 (*bcl6*) is a transcriptional repressor and participates in various physiological activities, including innate and adaptive immune responses and lymphocyte differentiation (Barish et al., 2010; Phan et al., 2005; Zhang et al., 2019b). Septins (*sept*) are an evolutionarily conserved family of guanosine-5'-triphosphate (GTP)-binding proteins, which play complex and important roles in host immune response to exogenous bacterial pathogens (Fu et al., 2016). Here, the SNP genotypes of the *ripk2*, *setp2*, *bcl6*, and *pkn2* genes were significantly changed in the WL population compared to the four farmed populations (Figure 7).

The availability of certain genomic resources, such as genome sequences and molecular markers, is still insufficient to improve the yield of economic species. Thus, there is an urgent need for an efficient method to explore the huge genetic diversity in germplasms to obtain target traits (Upadhyaya et al., 2011). Therefore, it is important to systematically assess and utilize germplasm resources by identifying allelic variations with significant impacts on important economic traits for fish improvement. In the present study, we found potential associations between candidate genes and important economic traits, such as growth (e.g., *psst1*, *grb10*, *bcar1*, *creb5*, *kcnmb2*, *klf9*, *sp4*, and *sp8*) and immunity (e.g., *ripk2*, *setp2*, *bcl6*, and *pkn2*). These candidate genes represent putative genomic landmarks that may be associated with traits of biological and commercial interest in farmed largemouth bass. These findings lay a foundation for the practical development of novel rapid-growing and disease-resistant varieties of largemouth bass.

CONCLUSIONS

Based on nucleotide diversity and heterozygosity analysis, we found that the genetic diversity of the improved domestic populations was lower than that of the introduced populations, providing a theoretical basis for the future breeding of largemouth bass. We detected several genomic regions putatively underlying selection in the five populations. These regions contained interesting candidate genes that may be associated with adaptive processes in captivity and traits of economic importance that have been targeted for selection. We also detected enrichment of several candidate genes

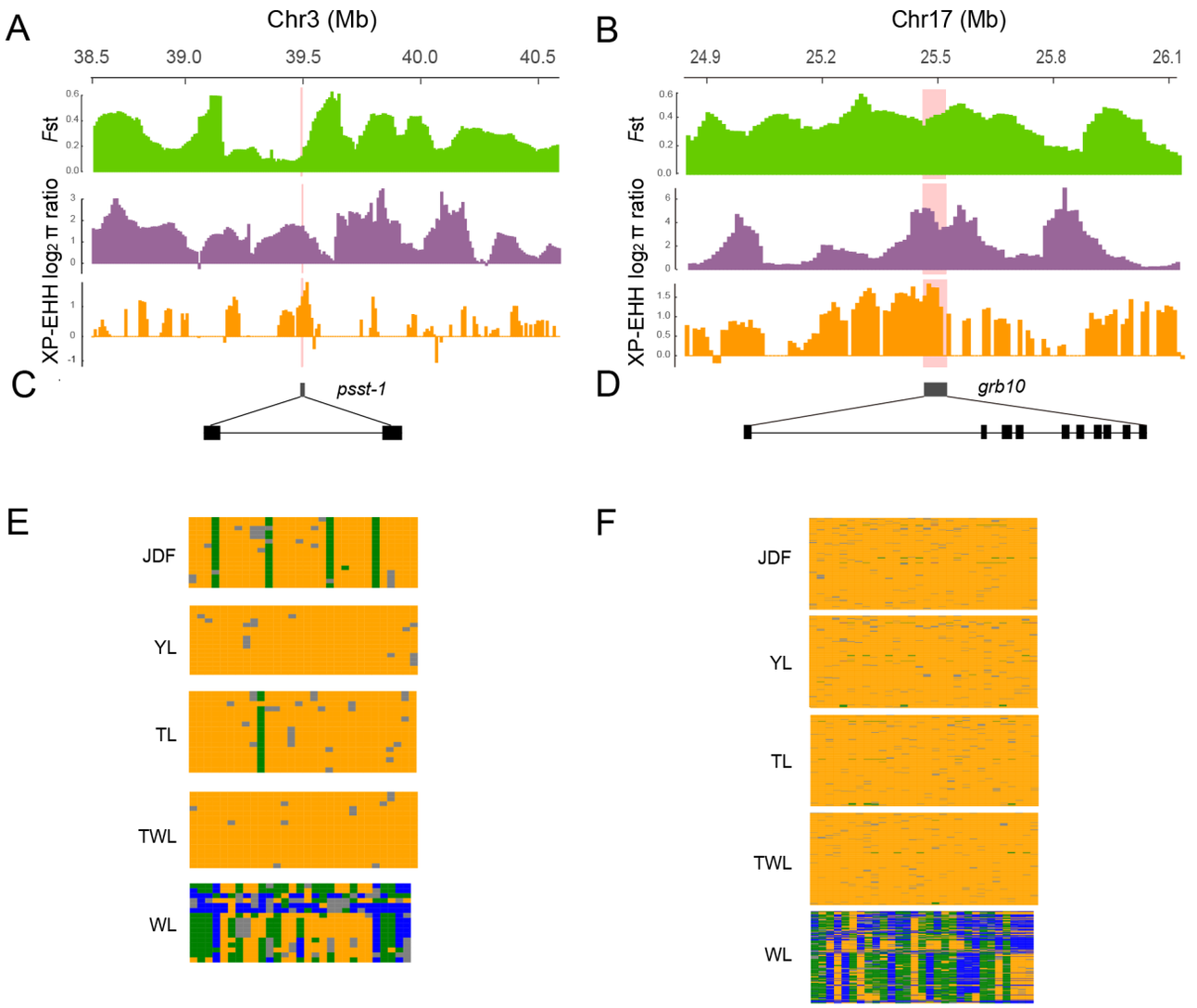

Figure 6 Selection signatures between domestic and imported populations

A–F: Preprosomatostatin 1 (*pss-1*) (A, C, E) and *grb10* (B, D, F) are examples of candidate genes with selection sweep signals. Three independent sets of signals (*F*st, π ratio, and XP-EHH) are shown along genomic regions in Chr3 (A) and Chr17 (B) covering two candidate genes, respectively. Middle panels (C, D) show structures of both genes (black rectangles are exons) in corresponding genomic regions. Lower panels show SNP allele distribution patterns along each gene (E, F) for five examined populations. Horizontal axis of each population represents examined individuals (30, except for WL *n*=29); vertical axis of each population shows detailed SNP allele distribution patterns (green, heterozygous site; orange, homozygous site of reference allele; blue, homozygous site of alternative allele; gray, missing data) among different individuals.

associated with production traits, growth, and disease resistance that are potentially important for genetic improvement. Our results provide a better understanding of the genes underlying traits of interest for practical aquaculture and the genomic effects of domestication in largemouth bass.

DATA AVAILABILITY

Raw reads from Illumina sequencing were deposited in the China National Genebank database (CNGBdb) under Accession No. CNP0003162, National Center for Biotechnology Information (NCBI) under BioProjectID PRJNA856472, Genome Sequence Archive (GSA) under Accession No. CRA013093, and Science Data Bank (SDB) under DOI:10.57760/sciencedb.03591.

SUPPLEMENTARY DATA

Supplementary data to this article can be found online.

COMPETING INTERESTS

The authors declare that they have no competing interests.

AUTHOR CONTRIBUTIONS

X.Y. and Q.S. conceived and designed the research. X.H.Z., C.F.S., J.J.D., and X.X.Y. performed data analyses. C.F.S., J.J.D., F.Y.G., H.T.Z., and Y.Y.T. prepared the samples. X.H.Z. and C.F.S. wrote the manuscript. Q.S. and X.Y. revised the manuscript. All authors read and approved the final version of the manuscript.

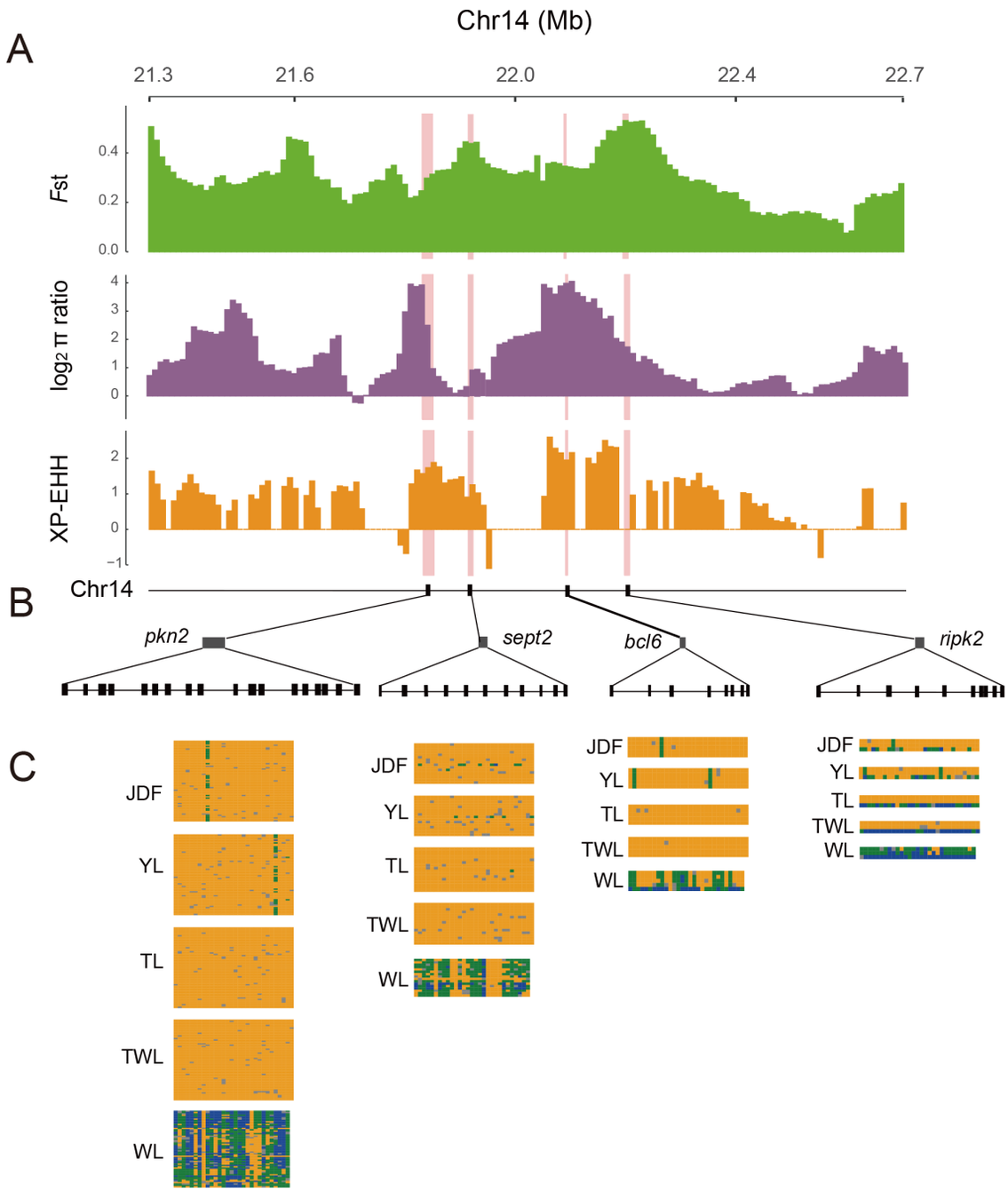

Figure 7 Selection signatures between domestic and imported populations

A–C: Four genes (*pkn2*, *sept2*, *bcl6*, and *ripk2*) were identified with selection sweep signals. Top panels (A) show three independent sets of signals (*F*st, π ratio, and XP-EHH) along genomic regions in Chr14 covering four candidate genes, respectively. Middle panels (B) show structures of four genes (black rectangles are exons) in corresponding genomic regions. Lower panels show SNP allele distribution patterns along each gene (C) for five examined populations. Horizontal axis of each population represents examined individuals (30, except for the WL *n*=29); vertical axis of each population shows detailed SNP allele distribution patterns (green, heterozygous site; orange, homozygous site of reference allele; blue, homozygous site of alternative allele; gray, missing data) among different individuals.

REFERENCES

Abraham G, Inouye M. 2014. Fast principal component analysis of large-scale genome-wide data. *PLoS One*, **9**(4): e93766.

Alexander DH, Novembre J, Lange K. 2009. Fast model-based estimation of ancestry in unrelated individuals. *Genome Research*, **19**(9): 1655−1664.

Bai JJ, Lutz-Carrillo DJ, Quan YC, Liang SX. 2008. Taxonomic status and genetic diversity of cultured largemouth bass *Micropterus salmoides* in China. *Aquaculture*, **278**(1–4): 27–30.

Barish GD, Yu RT, Karunasiri M, Ocampo CB, Dixon J, Benner C, et al. 2010. Bcl-6 and NF-κB cistromes mediate opposing regulation of the innate

immune response. *Genes & Development*, **24**(24): 2760−2765.
Baumung R, Simianer H, Hoffmann I. 2004. Genetic diversity studies in farm animals–a survey. *Journal of Animal Breeding and Genetics*, **121**(6): 361−373.
Ben-Shlomo A, Melmed S. 2010. Pituitary somatostatin receptor signaling. *Trends in Endocrinology & Metabolism*, **21**(3): 123−133.
Brazeau P, Vale W, Burgus R, Ling N, Butcher M, Rivier J, et al. 1973. Hypothalamic polypeptide that inhibits the secretion of immunoreactive pituitary growth hormone. *Science*, **5**(4068): 179:77−79.
Cádiz MI, López ME, Díaz-Domínguez D, Cáceres G, Yoshida GM, Gomez-Uchida D, et al. 2020. Whole genome re-sequencing reveals recent signatures of selection in three strains of farmed Nile tilapia (*Oreochromis niloticus*). *Scientific Reports*, **10**(1): 11514.
Cervia D, Bagnoli P. 2007. An update on somatostatin receptor signaling in native systems and new insights on their pathophysiology. *Pharmacology & Therapeutics*, **116**(2): 322−341.
Chen WK, Chen L, Zhang X, Yang N, Guo JH, Wang M, et al. 2022. Convergent selection of a WD40 protein that enhances grain yield in maize and rice. *Science*, **375**(6587): eabg7985.
Chen YX, Chen YS, Shi CM, Huang ZB, Zhang Y, Li SK, et al. 2018. SOAPnuke: a MapReduce acceleration-supported software for integrated quality control and preprocessing of high-throughput sequencing data. *GigaScience*, **7**(1): gix120.
Choy SH, Mahdy MAK, Al-Mekhlafi HM, Low VL, Surin J. 2015. Population expansion and gene flow in *Giardia duodenalis* as revealed by triosephosphate isomerase gene. *Parasites & Vectors*, **8**: 454.
Cingolani P, Platts A, Wang LL, Coon M, Nguyen T, Wang L, et al. 2012. A program for annotating and predicting the effects of single nucleotide polymorphisms, SnpEff: SNPs in the genome of Drosophila melanogaster strain w^{1118}; iso-2; iso-3. *Fly*, **6**(2): 80−92.
Danecek P, Auton A, Abecasis G, Albers CA, Banks E, DePristo MA, et al. 2011. The variant call format and VCFtools. *Bioinformatics*, **27**(15): 2156−2158.
Dong CJ, Jiang P, Zhang JF, Li XJ, Li SJ, Bai JJ, et al. 2019. High-density linkage map and mapping for sex and growth-related traits of largemouth bass (*Micropterus salmoides*). *Frontiers in Genetics*, **10**: 960.
Duan YX, Ouyang JH, Mo GX, Hao WJ, Zhang P, Yang HX, et al. 2022. Defensing role of novel piscidins from largemouth bass (*Micropterus salmoides*) with evidence of bactericidal activities and inducible expressional delineation. *Microbiological Research*, **256**: 126953.
Franke KR, Crowgey EL. 2020. Accelerating next generation sequencing data analysis: an evaluation of optimized best practices for Genome Analysis Toolkit algorithms. *Genomics & Informatics*, **18**(1): e10.
Frantz JD, Giorgetti-Peraldi S, Ottinger EA, Shoelson SE. 1997. Human GRB-IRβ/GRB10. Splice variants of an insulin and growth factor receptor-binding protein with PH and SH2 domains. *The Journal of Biological Chemistry*, **272**(5): 2659−2667.
Fu Q, Li Y, Yang YJ, Li C, Yao J, Zeng QF, et al. 2016. Septin genes in channel catfish (*Ictalurus punctatus*) and their involvement in disease defense responses. *Fish & Shellfish Immunology*, **49**: 110−121.
Gahete MD, Durán-Prado M, Luque RM, Martínez-Fuentes AJ, Quintero A, Gutiérrez-Pascual E, et al. 2009. Understanding the multifactorial control of growth hormone release by somatotropes: lessons from comparative endocrinology. *Annals of the New York Academy of Sciences*, **1163**(1): 137−153.
Gjedrem T, Robinson N. 2014. Advances by selective breeding for aquatic species: a review. *Agricultural Sciences*, **5**(12): 1152−1158.
Gutierrez AP, Yáñez JM, Davidson WS. 2016. Evidence of recent signatures of selection during domestication in an Atlantic salmon population. *Marine Genomics*, **26**: 41−50.
He WM, Rose DW, Olefsky JM, Gustafson TA. 1998. Grb10 interacts differentially with the insulin receptor, insulin-like growth factor I receptor, and epidermal growth factor receptor via the Grb10 Src homology 2 (SH2) domain and a second novel domain located between the pleckstrin homology and SH2 domains. *Journal of Biological Chemistry*, **273**(12): 6860−6867.
Kawakami Y, Esteban CR, Matsui T, Rodríguez-León J, Kato S, Belmonte JCI. 2004. *Sp8* and *Sp9*, two closely related buttonhead-like transcription factors, regulate *Fgf8* expression and limb outgrowth in vertebrate embryos. *Development*, **131**(19): 4763−4774.
Kon T, Pei LY, Ichikawa R, Chen CY, Wang P, Takemura I, et al. 2021. Whole-genome resequencing of large yellow croaker (*Larimichthys crocea*) reveals the population structure and signatures of environmental adaptation. *Scientific Reports*, **11**(1): 11235.
Larson G, Burger J. 2013. A population genetics view of animal domestication. *Trends in Genetics*, **29**(4): 197−205.
Lemopoulos A, Uusi-Heikkilä S, Huusko A, Vasemägi A, Vainikka A. 2018. Comparison of migratory and resident populations of brown trout reveals candidate genes for migration tendency. *Genome Biology and Evolution*, **10**(6): 1493−1503.
Letunic I, Bork P. 2021. Interactive Tree Of Life (iTOL) v5: an online tool for phylogenetic tree display and annotation. *Nucleic Acids Research*, **49**(W1): W293−W296.
Li H, Durbin R. 2009. Fast and accurate short read alignment with Burrows-Wheeler transform. *Bioinformatics*, **25**(14): 1754−1760.
Li H, Handsaker B, Wysoker A, Fennell T, Ruan J, Homer N, et al. 2009. The sequence alignment/map format and SAMtools. *Bioinformatics*, **25**(16): 2078−2079.
Li N, Zhou T, Geng X, Jin YL, Wang XZ, Liu SK, et al. 2018. Identification of novel genes significantly affecting growth in catfish through GWAS analysis. *Molecular Genetics and Genomics*, **293**(3): 587−599.
Liu F, Roth RA. 1995. Grb-IR: a SH2-domain-containing protein that binds to the insulin receptor and inhibits its function. *Proceedings of the National Academy of Sciences of the United States of America*, **92**(22): 10287−10291.
Liu JX, Cao DD, Liu YZ, Li Z, Si Y, Wang ZG, et al. 2018. Expression and functional analysis of receptor-interacting serine/threonine kinase 2 (RIP2) in Japanese flounder (*Paralichthys olivaceus*). *Fish & Shellfish Immunology*, **75**: 327−335.
López ME, Benestan L, Moore JS, Perrier C, Gilbey J, Di Genova A, et al. 2019. Comparing genomic signatures of domestication in two Atlantic salmon (*Salmo salar* L.) populations with different geographical origins. *Evolutionary Applications*, **12**(1): 137−156.
Lu K, Wei LJ, Li XL, Wang YT, Wu J, Liu M, et al. 2019. Whole-genome resequencing reveals *Brassica napus* origin and genetic loci involved in its improvement. *Nature Communications*, **10**(1): 1154.
Mäkinen H, Vasemägi A, McGinnity P, Cross TF, Primmer CR. 2015. Population genomic analyses of early-phase Atlantic Salmon (*Salmo salar*) domestication/captive breeding. *Evolutionary Applications*, **8**(1): 93−107.
Mastrochirico-Filho VA, del Pazo F, Hata ME, Villanova GV, Foresti F, Vera M, et al. 2019. Assessing genetic diversity for a pre-breeding program in *Piaractus mesopotamicus* by SNPs and SSRs. *Genes*, **10**(9): 668.
McCubrey JA, May WS, Duronio V, Mufson A. 2000. Serine/threonine phosphorylation in cytokine signal transduction. *Leukemia*, **14**(1): 9−21.
Nayfa MG, Jones DB, Benzie JAH, Jerry DR, Zenger KR. 2020. Comparing genomic signatures of selection between the Abbassa strain and eight wild

populations of Nile tilapia (*Oreochromis niloticus*) in Egypt. *Frontiers in Genetics*, **11**: 567969.

Nelson LE, Sheridan MA. 2005. Regulation of somatostatins and their receptors in fish. G*eneral and Comparative Endocrinology*, **142**(1–2): 117–133.

Phan RT, Saito M, Basso K, Niu HF, Dalla-Favera R. 2005. BCL6 interacts with the transcription factor Miz-1 to suppress the cyclin-dependent kinase inhibitor p21 and cell cycle arrest in germinal center B cells. *Nature Immunology*, **6**(10): 1054−1060.

Presnell JS, Schnitzler CE, Browne WE. 2015. KLF/SP transcription factor family evolution: expansion, diversification, and innovation in eukaryotes. *Genome Biology and Evolution*, **7**(8): 2289−2309.

Purcell S, Neale B, Todd-Brown K, Thomas L, Ferreira MAR, Bender D, et al. 2007. PLINK: a tool set for whole-genome association and population-based linkage analyses. *American Journal of Human Genetics*, **81**(3): 559−575.

Ravichandran G, Pasupuleti M, Arasu MV, Al-Dhabi NA, Arshad A, Arockiaraj J. 2020. Innate immune function of serine/threonine-protein kinase from *Macrobrachium rosenbergii* in response to host-pathogen interactions. *Fish & Shellfish Immunology*, **106**: 332−340.

Sabeti PC, Varilly P, Fry B, Lohmueller J, Hostetter E, Cotsapas C, et al. 2007. Genome-wide detection and characterization of positive selection in human populations. *Nature*, **449**(7164): 913−918.

Saraiva JL, Castanheira MF, Arechavala-López P, Volstorf J, Studer BH. 2018. Domestication and welfare in farmed fish. *In*: Teletchea F. Animal Domestication. London: IntechOpen.

Sheridan MA, Eilertson CD, Kerstetter TH. 1998. Changes in plasma somatostatin associated with seawater adaptation and stunting of coho salmon, *Oncorhynchus kisutch*. *Aquaculture*, **168**(1–4): 195–203.

Suebsong W, Poompuang S, Srisapoome P, Koonawootrittriron S, Luengnaruemitchai A, Johansen H, et al. 2019. Selection response for *Streptococcus agalactiae* resistance in Nile tilapia *Oreochromis niloticus*. *Journal of Fish Diseases*, **42**(11): 1553–1562.

Sun CF, Li J, Dong JJ, Niu YC, Hu J, Lian JM, et al. 2021. Chromosome‐level genome assembly for the largemouth bass *Micropterus salmoides* provides insights into adaptation to fresh and brackish water. *Molecular Ecology Resources*, **21**(1): 301−315.

Supp DM, Witte DP, Branford WW, Smith EP, Potter SS. 1996. Sp4, a member of the Sp1-family of zinc finger transcription factors, is required for normal murine growth, viability, and male fertility. *Developmental Biology*, **176**(2): 284−299.

Suske G. 1999. The Sp-family of transcription factors. *Gene*, **238**(2): 291−300.

Szpiech ZA, Hernandez RD. 2014. Selscan: an efficient multithreaded program to perform EHH-based scans for positive selection. *Molecular Biology and Evolution*, **31**(10): 2824−2827.

Tang L. 2020. Standardizing population genetics simulations. *Nature Methods*, **17**(9): 876−876.

Teletchea F. 2015. Domestication of marine fish species: update and perspectives. *Journal of Marine Science and Engineering*, **3**(4): 1227−1243.

Teletchea F. 2021. Fish domestication in aquaculture: 10 unanswered questions. *Animal Frontiers*, **11**(3): 87−91.

Tran NT, Gao ZX, Zhao HH, Yi SK, Chen BX, Zhao YH, et al. 2015. Transcriptome analysis and microsatellite discovery in the blunt snout bream (*Megalobrama amblycephala*) after challenge with *Aeromonas hydrophila*. *Fish & Shellfish Immunology*, **45**(1): 72–82.

Tsai HY, Hamilton A, Tinch AE, Guy DR, Gharbi K, Stear MJ, et al. 2015. Genome wide association and genomic prediction for growth traits in juvenile farmed Atlantic salmon using a high density SNP array. *BMC Genomics*, **16**: 969.

Upadhyaya HD, Reddy KN, Sharma S, Varshney RK, Bhattacharjee R, Singh S, et al. 2011. Pigeonpea composite collection and identification of germplasm for use in crop improvement programmes. *Plant Genetic Resources*, **9**(1): 97−108.

Van Bers NEM, Crooijmans RPMA, Groenen MAM, Dibbits BW, Komen J. 2012. SNP marker detection and genotyping in tilapia. *Molecular Ecology Resources*, **12**(5): 932−941.

Wang B, Qin CB, Zhang C, Jia JR, Sun CY, Li WS. 2014. Differential involvement of signaling pathways in the regulation of growth hormone release by somatostatin and growth hormone-releasing hormone in orange-spotted grouper (*Epinephelus coioides*). *Molecular and Cellular Endocrinology*, **382**(2): 851−859.

Wang SY, Kuang YY, Liang LQ, Sun B, Zhao XF, Zhang LM, et al. 2021a. Resequencing and SNP discovery of Amur ide (*Leuciscus waleckii*) provides insights into local adaptations to extreme environments. *Scientific Reports*, **11**(1): 5064.

Wang W, Ma CY, Ouyang LL, Chen W, Zhao M, Zhang FY, et al. 2021b. Genetic diversity and population structure analysis of *Lateolabrax maculatus* from Chinese coastal waters using polymorphic microsatellite markers. *Scientific Reports*, **11**(1): 15260.

Xu XY, Li XQ, Xu Z, Yao WX, Leng XJ. 2021. Dietary Azomite, a natural trace mineral complex, improved the growth, immunity response, intestine health and resistance against bacterial infection in largemouth bass (*Micropterus salmoides*). *Fish & Shellfish Immunology*, **108**: 53−62.

Ye X, Li WS, Lin HR. 2005. Polygenic expression of somatostatin in orange-spotted grouper (*Epinephelus coioides*): Molecular cloning and distribution of the mRNAs encoding three somatostatin precursors. *Molecular and Cellular Endocrinology*, **241**(1–2): 62–72.

Yin YH, Zhang XH, Wang XA, Li RH, Zhang YW, Shan XX, et al. 2021. Construction of a chromosome-level genome assembly for genome-wide identification of growth-related quantitative trait loci in *Sinocyclocheilus grahami* (Cypriniformes, Cyprinidae). *Zoological Research*, **42**(3): 262−266.

Yoshida GM, Barria A, Correa K, Cáceres G, Jedlicki A, Cadiz MI, et al. 2019. Genome-wide patterns of population structure and linkage disequilibrium in farmed nile tilapia (*Oreochromis niloticus*). *Frontiers in Genetics*, **10**: 745.

Yu JH, Schwartzbauer G, Kazlman A, Menon RK. 1999. Role of the Sp family of transcription factors in the ontogeny of growth hormone receptor gene expression. *Journal of Biological Chemistry*, **274**(48): 34327−34336.

Zeder MA. 2015. Core questions in domestication research. *Proceedings of the National Academy of Sciences of the United States of America*, **112**(11): 3191−3198.

Zhang C, Dong SS, Xu JY, He WM, Yang TL. 2019a. PopLDdecay: a fast and effective tool for linkage disequilibrium decay analysis based on variant call format files. *Bioinformatics*, **35**(10): 1786−1788.

Zhang GQ, Zhang XH, Ye HZ, Jiang SJ, Yu H, Li J, et al. 2018. Construction of high-density genetic linkage maps and QTL mapping in the golden pompano. *Aquaculture*, **482**: 90−95.

Zhang RS, Wu KY, Ke XM, Zhang XY, Xu GY, Shen H, et al. 2019b. *Bcl6aa* and *bcl6ab* are ubiquitously expressed and are inducible by lipopolysaccharide and polyI: C in adult tissues of medaka *Oryzias latipes*. *Journal of Experimental Zoology Part B*: *Molecular and Developmental Evolution*, **332**(1–2): 17–25.